JOURNAL OF VIROLOGY, Aug. 2003, p. 8765–8774 Vol. 77, No. 8
0022-538X/03/$08.00+0 DOI: 10.1128/JVI.77.16.8765–8774.2003

Alteration of Hepatitis A Virus (HAV) Particles by a Soluble Form of HAV Cellular Receptor 1 Containing the Immunoglobulin- and Mucin-Like Regions

Erica Silberstein,[1] Li Xing,[2] Willem van de Beek,[2] Jinhua Lu,[1] Holland Cheng,[2] and Gerardo G. Kaplan[1]*

Laboratory of Hepatitis and Related Emerging Agents, Division of Emerging and Transfusion Transmitted Diseases, Center for Biologics Evaluation and Research, Food and Drug Administration, Bethesda, Maryland 20892,[1] and Department of Biosciences, Karolinska Institute, Stockholm 14157, Sweden[2]

Received 23 December 2002/Accepted 23 May 2003

Hepatitis A virus (HAV) infects African green monkey kidney cells via HAV cellular receptor 1 (havcr-1). The ectodomain of havcr-1 contains an N-terminal cysteine-rich immunoglobulin-like region (D1), followed by a mucin-like region that extends D1 well above the cell surface. D1 is required for binding of HAV, and a soluble construct containing D1 fused to the hinge and Fc portions of human immunoglobulin G1 (IgG1), D1-Fc, bound and neutralized HAV inefficiently. However, D1-Fc did not alter the virions. To determine whether additional regions of havcr-1 are required to trigger uncoating of HAV, we constructed D1muc-Fc containing D1 and two-thirds of the mucin-like region fused to the Fc and hinge portions of human IgG1. D1muc-Fc neutralized 10 times more HAV than did D1-Fc. Sedimentation analysis in sucrose gradients showed that treatment of HAV with 20 to 200 nM D1muc-Fc disrupted the majority of the virions, whereas treatment with 2 nM D1muc-Fc had no effect on the sedimentation of the particles. Treatment of HAV with 100 nM D1muc-Fc resulted in low-level accumulation of 100- to 125S particles. Negative-stain electron microscopy analysis revealed that the 100- to 125S particles had the characteristics of disrupted virions, such as internal staining and diffuse edges. Quantitative PCR analysis showed that the 100- to 125S particles contained viral RNA. These results indicate that D1 and the mucin-like region of havcr-1 are required to induce conformational changes leading to HAV uncoating.

Hepatitis A virus (HAV) is an atypical member of the family *Picornaviridae* that causes acute hepatitis in humans (for a review, see reference 20). HAV has a positive-strand genomic RNA of approximately 7.5 kb that is covalently linked to a small virus-encoded VPg protein at its 5′ end (38) and contains a poly(A) tail at its 3′ end. The mature HAV capsid is formed by 60 copies of at least three viral proteins, VP1, VP2, and VP3. A small unmyristoylated protein, VP4, of 23 amino acids plays a signal role in capsid assembly (29) but has not been detected in mature virions. Nonstructural protein 2A remains associated with the structural proteins and serves as a signal for the assembly of pentamers, which are precursors involved in the morphogenesis of the capsid (29).

Wild-type HAV usually does not grow in cell culture. The virus was adapted to in vitro growth by serial passage in cell cultures of primate origin, which resulted in the establishment of persistent infections and attenuation (7, 8, 10, 12–14, 17, 30). HAV has also been adapted to growth in guinea pig, pig, and dolphin cell cultures (11), indicating that the cellular factors required for HAV replication are not restricted to primates.

Picornaviruses have different cell entry mechanisms. For instance, cellular receptors bind differently to a depression around the fivefold axis of poliovirus and the major group of rhinovirus (2, 18, 39) and induce conformational changes in the virions that result in the accumulation of 135S A particles and other uncoating intermediates (for a review, see reference 32). Foot-and-mouth disease virus binds to integrin receptors through an RGD motif present in the G-H loop of VP1 (21) without triggering the formation of A particles, enters the endosomes, and uncoats in the acidic environment of this compartment (28). Another interesting example of the cell entry mechanism diversity in the family *Picornaviridae* is that of the minor group of rhinovirus, which binds low-density lipoprotein receptors at the star-shaped dome on the fivefold axis rather than in the canyon (19) and are internalized into acidic endosomes for uncoating (33). Little is known about the cell entry mechanism of HAV, which cannot be inferred from other members of the family *Picornaviridae* because of the atypical characteristics of HAV and the diverse cell entry modes of members of the family. We have previously shown that HAV binds to a cell surface receptor identified in African green monkey kidney cells as HAV cellular receptor 1 (havcr-1) (24). Nucleotide sequence analysis revealed that havcr-1 is a class I integral membrane glycoprotein with an extracellular domain containing an N-terminal immunoglobulin-like cysteine-rich region (D1), followed by a threonine-, serine-, and proline-rich region that most likely extends D1 well above the cell surface. havcr-1 and its human homolog huhavcr-1 are very similar and have HAV receptor function in common (16, 24).

Although the natural function of havcr-1 remains unknown, McIntire et al. (27) identified a family of murine orthologs of havcr-1, termed TIM, as asthma susceptibility genes. Interestingly, it has been shown that there is an inverse relationship

* Corresponding author. Mailing address: Laboratory of Hepatitis and Related Emerging Agents, DETTD, CBER, FDA, 8800 Rockville Pike, Bldg. 29, HFM-325, Bethesda, MD 20892. Phone: (301) 496-0338. Fax: (301) 480-7928. E-mail: GK@helix.nih.gov.

between HAV infection and the development of atopy (25, 26), which could be explained by a modification of the Th2 response triggered by the HAV infection (37). Because the incidence of HAV infection is reduced in industrialized countries, these findings may explain the large increase in asthma prevalence in those countries over the last 20 years (27). Therefore, if the association between HAV infection and atopy is confirmed, the current practice of vaccinating children against HAV will need to be reassessed.

We previously showed that D1 and its first N-glycosylation site are required for binding of HAV (35) to havcr-1. We also showed that D1 fused to the hinge and Fc portions of human immunoglobulin G1 (IgG1), D1-Fc, binds and neutralizes HAV (34). However, our preliminary studies indicated that D1-Fc does not induce HAV conformational changes leading to uncoating of the viral genome. In this paper, we show that D1 plus the mucin-like region of havcr-1 fused to the hinge and Fc regions of human IgG1 (D1muc-Fc) neutralized HAV more efficiently than did D1-Fc and disrupted the viral particles. Electron microscopic (EM) analysis of negatively stained HAV showed that the altered particles had diffused edges and were internally stained, which is characteristic of altered particles. These results indicate that D1 and the mucin-like region of havcr-1 are required to induce alteration and uncoating of HAV.

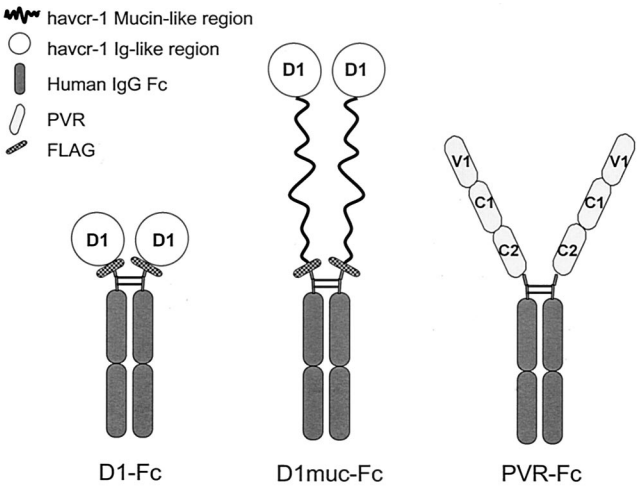

FIG. 1. Schematic representation of immunoadhesins D1-Fc, D1muc-Fc, and PVR-Fc. D1-Fc contains the cysteine-rich region of havcr-1 (D1) tagged at the N terminus with peptide DTKDDDDK (FLAG) and fused to the hinge and Fc regions of human IgG1 (34). PVR-Fc contains the ectodomain of pvr, the poliovirus receptor, with its three Ig-like domains (V1, C1, and C2) fused to the hinge and Fc regions of human IgG1 (34). To construct D1muc-Fc, D1 and two-thirds of the mucin-like region were tagged at the N terminus with the FLAG peptide and fused to the hinge and Fc regions of human IgG1. The fusion proteins form homodimers linked by the Fc disulfide bonds.

MATERIALS AND METHODS

Antisera. Guinea pig anti-HAV antibody produced in rabbits immunized with heat-disrupted HAV particles was a gift of S. Feinstone, Food and Drug Administration. Anti-HAV serum was produced in rabbits immunized with commercially available HAV vaccine (34).

Murine IgG1 monoclonal antibodies (MAbs) 190/4, directed against havcr-1 (24), and M2, directed against the FLAG peptide DTKDDDDK (Kodak), were purified through affinity columns. Unlabeled human anti-HAV polyclonal antiserum was obtained from the HAVAB kit (Abbott Laboratories). Goat anti-human Fc antibodies, phosphatase-labeled goat anti-human IgG antibodies, phosphatase-labeled goat anti-mouse IgG antibodies, phosphatase-labeled goat anti-guinea pig IgG antibodies, and peroxidase-labeled rabbit anti-human Fc antibodies were used as suggested by the manufacturer (Kirkegaard & Perry Laboratories, Inc.).

Cells and viruses. Fetal rhesus monkey kidney (FRhK-4) cells were a gift of S. Emerson, National Institutes of Health. Cells were grown in monolayer cultures in Eagle's minimal essential medium (EMEM) supplemented with 10% horse serum.

Continuous clone GL37 of African green monkey kidney (AGMK) cells (36), termed AGMK GL37 cells, was grown in EMEM with 10% fetal bovine serum (FBS) at 37°C in a CO_2 incubator.

Chinese hamster ovary (CHO) cells deficient in the enzyme dihydrofolate reductase ($dhfr^-$) were obtained from the American Type Culture Collection and expanded in growth medium consisting of Iscove's medium containing 10% FBS and supplemented with 100 μM hypoxanthine and 16 μM thymidine (Sigma Chemical Co.). CHO cell transfectants expressing the hamster *DHFR* minigene were selected in Iscove's medium containing 10% dialyzed FBS with no supplement (selection medium).

Cell culture-adapted strain HM175 of HAV was derived from infectious cDNA (7), passaged approximately 100 times in BS-C-1 cells, and termed HAV PI. Virus stocks were prepared by growing HAV PI in FRhK-4 cells. After 10 days, culture supernatants were collected and clarified by centrifugation. Cell culture-adapted strain KRM003 of HAV, which we termed KRM003 HAV, was grown in GL37 cells (36).

A sucrose-purified cytopathic variant of cell culture-adapted strain HM175 of HAV (9), which we termed cytopathic HAV, was obtained from Viral Antigens, Inc.

HAV titer determination. Cytopathic HAV was titrated on 96-well plates containing confluent monolayers of FRhK-4 cells. Eight to 16 replicate wells were inoculated with 100 μl of 10-fold dilutions of HAV prepared in EMEM–10% FBS. Plates were incubated at 35°C for 10 days in a CO_2 incubator. Cytopathic effect was assessed under a microscope, and viral titers were calculated by the method of Reed and Muench (31).

HAV PI was titrated by an endpoint assay in 96-well plates containing confluent monolayers of AGMK GL37 cells (34). Briefly, 8 to 16 replicate wells were inoculated with 100 μl of 10-fold dilutions of HAV and incubated at 35°C for 2 weeks in a CO_2 incubator. Cells were fixed with 95% methanol, and HAV was detected by enzyme-linked immunosorbent assay (ELISA). Wells that developed at least 2.5 times the color of uninfected control wells were considered positives, and viral titers were calculated by the Reed and Muench method (31).

Plasmids. A plasmid coding for the Ig-like region and two-thirds of the mucin-like region of havcr-1 fused to the Fc and hinge fragments of human IgG1 (D1muc-Fc) was constructed and termed pEF-D1muc-Fc. The cDNA fragment coding for D1 in pEF-HAVcr-1D1flag (34) was replaced with a cDNA PCR fragment amplified from pDR2GL37/5 (24) coding for D1 plus two-thirds of the mucin-like region of havcr-1 (amino acids 1 to 281). The PCR was performed in 20 cycles with the *Taq* and *Pwo* DNA polymerases from the Expand High Fidelity PCR System (Roche Laboratories) as recommended by the manufacturer. Synthetic oligonucleotide D1/*Sal*I (5′-CGGATACCCGTCGACATAATGCATCTT CAAGTGGTCATC-3′), coding for a *Sal*I site before the initiation codon of havcr-1, followed by nucleotides 198 to 216 of the havcr-1 cDNA, was used as the positive-sense PCR primer. Synthetic oligonucleotide D1muc/flag/*Spe*I (5′-GG ACTAGTACTCACCCTTGTCATCGTCGTCCTTGTAGTCGTCTGTTGAG AAGGTTGTTGTTGTTGAGACGGTTGCTGTTGGTAGCAAAGA-3′), containing an *Spe*I site, followed by an artificial splicing donor signal (GTGAGT), 24 nucleotides coding for the FLAG peptide DTKDDDDK, and nucleotides 1022 to 986 of the havcr-1 cDNA, was used as the negative-sense PCR primer. The unique band produced in the PCR was purified by Tris-acetate-EDTA–1% low-melting-point agarose gel electrophoresis, cut with *Sal*I and *Spe*I, ligated into *Sal*I/*Spe*I-cut and phosphatase-treated pEF-HAVcr-1D1flag, and used to transform *Escherichia coli* DH5α. The nucleotide sequence of a plasmid that had the expected restriction pattern of pEF-D1muc-Fc was verified with an ABI Prism automatic sequencer and the ABI Prism Dye terminator cycle-sequencing ready reaction kit (Perkin-Elmer Cetus, Inc.).

Production of soluble receptor forms. Expression and purification of immunoadhesins coding for the hinge and Fc portions of human IgG1 fused to D1 (D1-Fc) and the ectodomain of the poliovirus receptor (PVR-Fc) have been described previously (34). Figure 1 shows a schematic representation of D1-Fc and PVR-Fc compared to D1muc-Fc. D1muc-Fc was expressed in CHO cells as described for D1-Fc and PVR-Fc (34). Briefly, $dhfr^-$ CHO cell monolayers were

cotransfected with 0.45 μg of pDHIP and 3.5 μg of pEF-D1muc-Fc with the Fugene6 reagent as recommended the manufacturer (Roche Laboratories). CHO cells were incubated for 14 days in selection medium consisting of Iscove's medium containing 10% FBS, and transfectants were cloned by endpoint dilution in 96-well plates. D1muc-Fc expressed in the supernatant of the CHO transfectants was assayed by capture ELISA in 96-well plates coated with goat anti-human Fc antibody and staining with peroxidase-labeled rabbit anti-human Fc conjugate. To produce higher levels of secreted soluble receptor, clones expressing D1muc-Fc were treated with increasing concentrations of methotrexate to a maximum of 5 μM. To purify D1muc-Fc, CHO cell transfectants expressing the highest levels of the soluble receptor were grown in 2,100-cm^2 hollow-fiber bioreactors (FiberCell Systems Inc.) at 37°C in a CO_2 incubator. Bioreactors were inoculated with 2×10^8 cells and grown in selection medium containing 5 μM methotrexate and 2% dialyzed FBS. Lactic acid production rates in the culture medium were monitored every day. The medium from the extracapillary space (60 ml) containing the soluble receptor was harvested every 2 days. D1muc-Fc was purified from 250 ml of medium by affinity chromatography with a 2-ml column of Affi-Gel protein A-agarose (Bio-Rad Laboratories) as recommended by the manufacturer. D1muc-Fc was eluted at pH 3 in 20 1-ml fractions that were neutralized with 300 μl of 1 M Tris-HCl (pH 9.0) per fraction. Fractions containing D1muc-Fc were identified by dot blot analysis staining with phosphatase-labeled anti-human Fc antibodies. Eluted fractions were also analyzed by SDS-PAGE with Novex Tris-glycine–4 to 20% polyacrylamide gels (Invitrogen) and staining with Coomassie blue.

Western blot analysis. Samples containing purified D1-Fc, D1muc-Fc, and PVR-Fc were resolved by denaturing SDS-PAGE in Novex Tris-glycine–4 to 20% polyacrylamide gels, transferred to polyvinylidene fluoride membranes (Immobilon-P; Millipore, Inc.), and stained with a 1:1,000 dilution of goat anti-human Fc antibody and a 1:5,000 dilution of phosphatase-labeled rabbit anti-goat antibody or with 1 μg of MAb M2 per ml and a 1:1,000 dilution of phosphatase-labeled anti-mouse IgG antibody. The substrate 5-bromo-4-chloro-3-indolylphosphate (BCIP)–nitroblue tetrazolium (Kirkegaard & Perry Laboratories) was used as recommended by the manufacturer.

Neutralization assays. HAV PI (10^5 50% tissue culture infective doses [$TCID_{50}$]) was incubated with 50 μg of purified D1-Fc, D1muc-Fc, or PVR-Fc overnight at 4°C in 500 μl of EMEM–10% FBS. Tenfold dilutions of the neutralization reaction mixtures were titrated in 96-well plates containing confluent monolayers of AGMK GL37 cells. Each dilution was inoculated in 8 to16 wells, and the virus was adsorbed for 4 h at 37°C in a CO_2 incubator. After washing three times with EMEM, 200 μl of EMEM–10% FBS was added per well and the plates were incubated at 35°C under CO_2 for 10 days. Cells were fixed with 90% methanol, and HAV titers were determined by ELISA (34).

To determine the specificity of the soluble-receptor-mediated neutralization of HAV, 10 μg of purified D1muc-Fc or PVR-Fc was treated with 30 μg of MAb 190/4 or control MAb M2 for 2 h at 4°C, followed by the addition of 10^5 $TCID_{50}$ of cytopathic HAV and further overnight incubation at 4°C. Confluent monolayers of FRhK-4 cells in 96-well plates were inoculated with 100 μl of 10-fold dilutions of the neutralization reaction mixtures per well. Each dilution was inoculated into 32 wells, and the plates were incubated for 4 h at 37°C. After washing three times with EMEM, 200 μl of EMEM–10% FBS was added per well and the plates were incubated at 35°C under CO_2 for 10 days. Cytopathic effect was assessed under a microscope, and viral titers were calculated by the method of Reed and Muench (31).

Sedimentation analysis of HAV particles. HAV virions were purified by sedimentation in linear 15 to 30% sucrose gradients with a Beckman SW41 rotor at 4°C for 100 min at 40,000 rpm. Gradients were collected from the bottom in 20 fractions of 0.5 ml each, and HAV was detected by ELISA (34). The 160S virion peak was pooled and stored at −70°C. Sucrose-purified HAV virions were treated with different amounts of PVR-Fc or D1muc-Fc and analyzed by ultracentrifugation in 15 to 30% sucrose gradients as indicated above. To minimize the loss of material, incubation of HAV with soluble receptors was done in siliconized tubes. Under these experimental conditions, we observed a consistent loss of about 30% of the material. This sedimentation analysis was repeated at least three times with similar results. Alternatively, fractions were immunoprecipitated with rabbit anti-HAV antibodies. Seventy microliters of MagnaBind goat anti-rabbit IgG beads (Pierce) was incubated for 2 h at 4°C with 2 μl of rabbit anti-HAV antibodies, 500 μl of each sucrose gradient fraction, and 600 μl of PBL buffer (0.1% sodium dodecyl sulfate [SDS], 1% sodium deoxycholate, 1% Triton X-100, 0.05% sodium azide). After extensive washing, immunoprecipitated proteins were analyzed by Western blotting and developed with a 1:2,000 dilution of guinea pig anti-HAV antibody and a 1:1,000 dilution of phosphatase-labeled goat anti-guinea pig IgG antibody.

^{35}S-labeled poliovirus (22) was used as a sedimentation marker, and 160S virions and 80S empty particles were identified by scintillation counting.

Quantitative RT-PCR. To quantitate the HAV RNA in each sucrose gradient fraction, 10 μl of each fraction was diluted with 200 μl of water and boiled for 5 min to release the viral RNA and 10 μl of the sample was used for reverse transcription (RT)-PCR. To quantitate the HAV RNA in pooled fractions, RNA was extracted with phenol and precipitated with ethanol. HAV RNA was quantitated by *Taq*Man with the Platinum Quantitative RT-PCR ThermoScript one-step RT-PCR system as suggested by the manufacturer (Invitrogen). A 0.2 μM concentration of HAV positive-sense primer 5′-GGCATTTAGGTTTTTCCTC ATTCTTA-3′, corresponding to nucleotides 685 to 710, and negative-sense primer 5′-AATGTCTGCCAAAGACAGGATGT-3′, corresponding to HAV nucleotides 770 to 792, was used in the PCR. To detect the amplification product, 10 μM HAV fluorogenic probe [5′-(6FAM)CAAGGTATTTTCCAGACTGTT GGGAGTGGTCT(TAMRA)-3′], corresponding to nucleotides 733 to 764, was added to the PCR mixture. The incubation conditions used were 30 min at 50°C (RT), 10 min at 95°C, and 40 cycles of 15 s at 95°C and 1 min at 60°C (amplification reaction). Full-length HAV RNA transcribed from linearized pT7HAV was synthesized with T7 RNA polymerase (40) and used as the standard for the quantitative PCR.

Analysis of HAV particles by EM. Fractions from five replicate 15 to 30% sucrose gradients containing cytopathic HAV treated with D1muc-Fc were pooled and concentrated with Centricon 30 (Amicon) to a final volume of 50 μl. HAV treated with PVR-Fc and sedimented in a parallel 15 to 30% sucrose gradient was used as a control. Samples (3 μl) of pooled fractions were mounted on carbon-coated copper grids and stained with 2% uranyl acetate for 15 s. After being rinsed with water, samples were examined at a magnification of ×45,000 in a Philips CM120 electron microscope. Alternatively, sucrose-purified KRM003 HAV virions were treated with 30 μg of D1muc-Fc for 10, 30, or 60 min, mounted on grids directly without sedimentation, stained as indicated above, and examined under the electron microscope at a magnification of ×17,000.

RESULTS

Expression of D1muc-Fc in CHO cells. We previously showed that D1-Fc, a recombinant protein containing the Ig-like region of havcr-1 fused to the human IgG1 Fc and hinge portions, bound and neutralized HAV inefficiently (34). To determine whether the mucin-like region of havcr-1 is needed to enhance HAV receptor function, we constructed D1muc-Fc, a soluble receptor containing D1 plus two-thirds of the mucin-like region of havcr-1 fused to the hinge and Fc regions of human IgG1. A FLAG tag epitope was inserted between the mucin-like region and the IgG1 fragment to monitor the expression of the fusion protein with anti-FLAG MAb M2. A schematic representation of D1-Fc, D1muc-Fc, and control PVR-Fc, which contains the ectodomain of the poliovirus receptor fused to the same hinge and Fc fragments, is shown in Fig. 1. D1muc-Fc was overexpressed in $dhfr^-$ CHO cells. Transfectants that secreted approximately 10 μg of D1muc-Fc per ml into the cell culture supernatant were cultured in hollow-fiber bioreactors. The bioreactors' extracapillary space supernatant (60 ml) was harvested every 2 days. Approximately 1 to 2.5 mg of D1muc-Fc was purified from four bioreactor harvests by affinity chromatography with protein A-agarose columns. SDS-polyacrylamide gel electrophoresis (PAGE) analysis (Fig. 2A) showed that purified D1muc-Fc migrated as a single band of 95 kDa (lane 1), control PVR-Fc (lane 2) migrated as a single band of 87 kDa, and D1-Fc contained several bands with the fully glycosylated form (arrow, lane 3) migrating as a 50-kDa band (34). Western blot analysis (Fig. 2B) showed that the D1muc-Fc 95-kDa band reacted with the anti-FLAG MAb M2 (lane 1) and anti-human Fc antibodies (lane 4). As expected, D1-Fc reacted with both antibodies (lanes 3 and 6) whereas PVR-Fc, which does not contain a

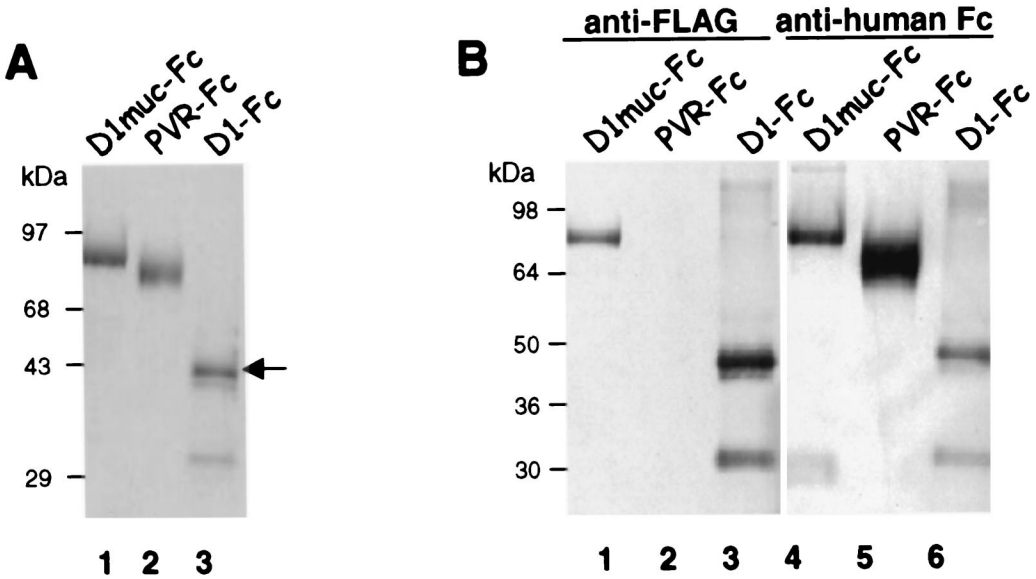

FIG. 2. Expression of immunoadhesins in CHO cells. (A) The immunoadhesins D1-Fc, D1muc-Fc, and PVR-Fc were purified with protein A columns. The eluted immunoadhesins were analyzed by denaturing SDS-PAGE in 4 to 20% polyacrylamide gels and stained with Coomassie blue. The arrow points to the fully glycosylated form of D1-Fc. (B) Protein A-purified D1muc-Fc (lanes 1 and 4), PVR-Fc (lanes 2 and 5), and D1-Fc (lanes 3 and 6) were analyzed by denaturing SDS-PAGE in a 4 to 20% polyacrylamide gel, transferred to a polyvinylidene difluoride membrane, and probed with anti-FLAG MAb M2 (lanes 1 to 3) or anti-human Fc antibodies (lanes 4 to 6). The positions of prestained molecular size markers and their sizes in kilodaltons are shown.

FLAG epitope, reacted only with the anti-human Fc antibodies (lane 5). These data confirmed that the CHO transfectants expressed D1muc-Fc of the expected size and antigenicity.

Efficient neutralization of HAV by D1muc-Fc. Since D1-Fc contains only D1 and neutralizes HAV inefficiently (34), we hypothesized that D1muc-Fc, a construct containing D1 plus the mucin-like region of havcr-1, could neutralize HAV more efficiently because of the presence of the mucin-like region. To test this theory, we treated 10^5 $TCID_{50}$ of HAV PI with 50 μg of D1-Fc, D1muc-Fc, or control PVR-Fc and compared the neutralization efficiencies of the different soluble receptors. After 2 h of incubation at 37°C, residual infectious virus was titrated in 96-well plates containing confluent monolayers of AGMK GL37 cells. The 96-well plates were incubated at 35°C under CO_2 for 2 weeks, cells were fixed, and viral titers were determined by ELISA with anti-HAV antibodies (Fig. 3). PVR-Fc had no effect on viral titers, whereas treatment with D1-Fc and D1muc-Fc neutralized approximately 0.6 and 1.6 logs of HAV, respectively. This 10-fold increase in the efficiency of neutralization of HAV indicated that the mucin-like region of havcr-1 plays a role in HAV receptor function.

MAb 190/4 blocks neutralization of HAV by D1muc-Fc. We previously showed that anti-havcr-1 protective MAb 190/4 blocks binding of HAV to havcr-1 and protects GL37 cells against infection (24). MAb 190/4 also reacted with D1-Fc and inhibited the binding and neutralization of HAV (34). To determine whether MAb 190/4 can react with D1muc-Fc and block HAV neutralization, we first treated 10 μg of D1muc-Fc or PVR-Fc with 30 μg of MAb 190/4 or control MAb M2 for 2 h at 4°C and then incubated the reaction mixture with 10^5 $TCID_{50}$ of cytopathic HAV. The residual infectious HAV was titrated in 96-well plates containing FRhK-4 cells, a rhesus monkey kidney cell line that expresses an antigenic variant of havcr-1 that does not react with MAb 190/4 (15). Therefore, the MAb 190/4 present in the neutralization reaction mixture did not protect FRhK-4 cells against HAV infection. At 10 days postinfection, the cytopathic effect was visualized under a microscope to determine HAV titers. Under these experimental conditions with cytopathic HAV, D1muc-Fc neutralized approximately 1 log of HAV whereas PVR-Fc had no effect on HAV titers (Fig. 4). Neutralization of HAV was blocked by

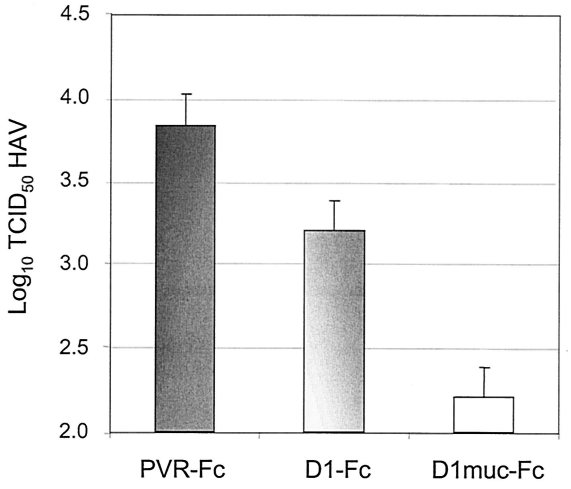

FIG. 3. Neutralization of HAV by soluble receptors. HAV PI (10^5 $TCID_{50}$) was neutralized with 50 μg of purified D1-Fc, D1muc-Fc, or PVR-Fc overnight at 4°C. Residual infectious HAV was titrated by endpoint dilution in 96-well plates containing confluent monolayers of GL37 cells. HAV titers were determined by ELISA. Values are the $\log_{10}$ of the HAV titers determined by the Reed and Muench method (31), and the standard deviations are shown as error bars.

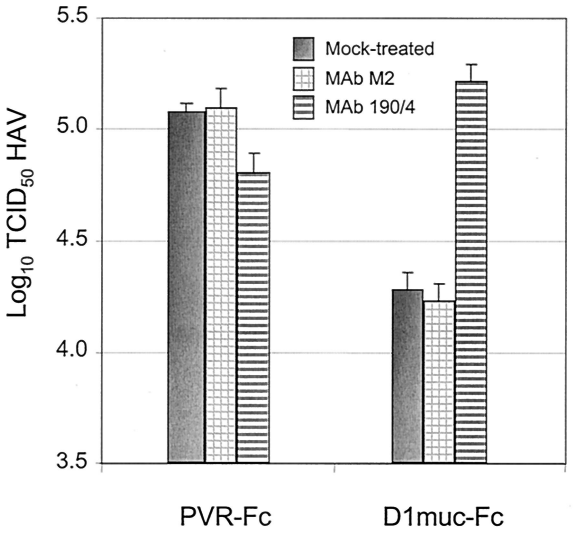

FIG. 4. Inhibition of D1muc-Fc-mediated neutralization of HAV by protective MAb 190/4. Equal amounts (10 μg) of D1muc-Fc and PVR-Fc were treated with 30 μg of MAb 190/4 or control MAb M2 for 2 h at 4°C and then incubated with 10^5 $TCID_{50}$ of cytopathic HAV. Residual infectious HAV was titrated by endpoint dilution in 96-well plates containing FRhK-4 cells. The cytopathic effect was visualized under a microscope at 10 days postinfection. The values shown are the log_{10} of the HAV titers determined by the Reed and Muench method (31), and the standard deviations are shown as error bars.

treatment with MAb 190/4 but not by treatment with control MAb M2, which binds to the FLAG tag introduced at the C terminus of the mucin-like region. As expected, PVR-Fc had no significant effect on the HAV titers, regardless of the MAb treatment. This blocking experiment clearly demonstrated that the interaction of D1muc-Fc with HAV is specific and mimics the interaction of the virus with havcr-1 expressed at the cell surface.

D1muc-Fc induces conformational changes in HAV. The mechanism of neutralization of HAV by soluble receptors was studied by sedimentation analysis in sucrose gradients. Purified HAV virions were incubated with 50 μg of PVR-Fc, D1-Fc, or D1muc-Fc for 2 h at 37°C and loaded onto linear 15 to 30% sucrose gradients. The gradients were ultracentrifuged at 4°C in an SW40 rotor at 40,000 rpm for 100 min and collected from the bottom in 20 fractions. The sedimentation profile of the HAV particles was determined by capture ELISA (34). [^{35}S]methionine-labeled poliovirus particles run in parallel gradients were used as 160S and 80S sedimentation markers. Treatment of HAV with PVR-Fc had no effect on the sedimentation of the virions (Fig. 5A), which migrated in the same position as mock-treated HAV particles (data not shown). Treatment with D1-Fc induced a minor shift in the sedimentation of HAV. This minor shift was observed in three separate experiments and is consistent with the inefficient binding and neutralization of HAV induced by D1-Fc (34). Surprisingly, treatment of HAV with 50 μg of D1muc-Fc resulted in complete loss of the 160S particles, which suggested that D1muc-Fc triggered the disruption of the HAV virions. The lack of detection of disrupted HAV particles and viral subunits in the gradients was puzzling. However, it is possible that the disrupted viral particles were unstable or that the antibodies used in the ELISA do not react with the generated viral subunits. An alternative interpretation of the soluble-receptor-mediated disruption of the viral particles is that biding of D1muc-Fc prevented the detection of HAV in the capture ELISA. Unfortunately, we were unable to directly test this theory with a titration assay because D1muc-Fc is very sticky and significantly increased the background levels of the ELISA (data not shown). To circumvent this problem, we analyzed the sedimentation of viral particles with a real-time one-step *Taq*Man RT-PCR assay to quantitate HAV genomes (Fig. 5B). This *Taq*Man assay can identify viral particles containing HAV RNA, including those that could have escaped detection in the capture ELISA. In the PVR-Fc gradient, we detected a peak of HAV RNA in fractions corresponding to 160S particles, which is consistent with the peak of HAV particles detected by the capture ELISA (compare Fig. 5A and B). However, in the D1muc-Fc gradient, we did not detect significant levels of HAV RNA in any of the fractions, which is consistent with the lack of HAV-specific signal observed in the capture ELISA (compare Fig. 5A and B). These *Taq*Man assay results further confirmed our initial hypothesis that D1muc-Fc disrupted the HAV particles.

To verify that the loss of the HAV 160S particles was not due to the formation of aggregates that accumulated at the bottom of the tubes, gradient pellets were resuspended and evaluated by ELISA. Similar levels of HAV were found in the pellets of PVR-Fc- and D1muc-Fc-treated samples (data not shown), which confirmed that the D1muc-Fc-treated HAV particles were not preferentially pelleted.

To further characterize the interaction of HAV with D1muc-Fc, virions were incubated with different amounts of D1muc-Fc for 2 h at 37°C and sedimented in 15 to 30% sucrose gradients (Fig. 5C). Treatment of HAV with 0.2 μg (0.002 μM) of D1muc-Fc did not affect the sedimentation profile of the virions, whereas treatment with 2 μg (0.02 μM), 10 μg (0.1 μM), and 20 μg (0.2 μM) of D1muc-Fc disrupted the majority of the 160S HAV particles. Interestingly, treatment of HAV with 10 μg (0.1 μM) of D1muc-Fc resulted in low-level accumulation of 100- to 125S particles (fractions 10 to 12). To determine whether D1muc-Fc induced the disruption of HAV particles in a concentration-dependent manner, we performed a finer titration between 0.2 and 2 μg of soluble receptor under the same experimental conditions (Fig. 5D). The level of disrupted HAV particles was proportional to the amount of D1muc-Fc used in the reaction mixture, with intermediate disruption levels observed at 0.5 and 1 μg of soluble receptor. It should be pointed out that the low-level absorbance in fractions 17 to 20 at the top of the gradients, which was less than two times the background level, was not due to HAV antigens from disrupted particles since gradients containing only soluble-receptor preparations gave similar absorbance levels (data not shown). Our data clearly show that D1muc-Fc induced the disruption of HAV particles in a concentration-dependent manner.

Characterization of the 100- to 125S particles by Western blotting and *Taq*Man analysis. The 100- to 125S particles were further characterized by Western blot analysis. HAV was treated with 10 μg of D1muc-Fc or PVR-Fc and analyzed in sucrose gradients as indicated above (Fig. 6A). Fractions 4 to 20 of the gradients were immunoprecipitated with rabbit anti-

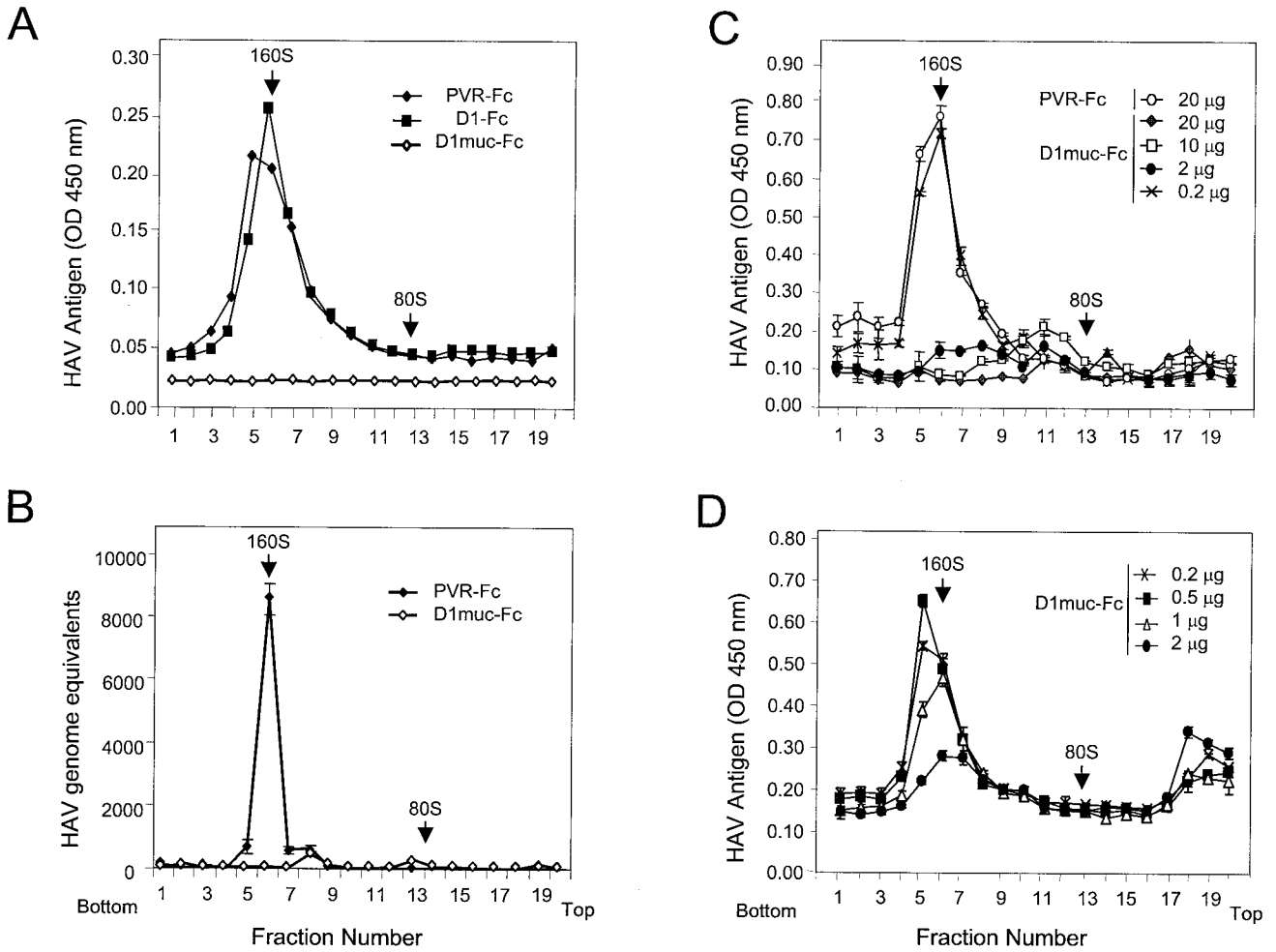

FIG. 5. Sedimentation analysis of HAV treated with soluble receptors. (A) Purified cytopathic HAV virions were incubated with 50 μg of PVR-Fc, D1-Fc, or D1muc-Fc for 2 h at 37°C and loaded onto linear 15 to 30% sucrose gradients. After ultracentrifugation at 4°C for 100 min with an SW40 rotor at 40,000 rpm, gradients were collected from the bottom in 20 fractions. HAV antigen in the fractions was determined by capture ELISA. The data shown are mean results from duplicate wells; duplicate values varied by less than 10%. (B) Aliquots (10 μl) of each fraction from a gradient similar to that shown in panel A were diluted in 200 μl of water and boiled, and 10 μl was used as a template with which to quantitate HAV RNA with a one-step real-time *Taq*Man RT-PCR assay. In vitro-synthesized full-length HAV RNA was used as the standard for the quantitative PCR. The data shown are mean results from triplicate reactions. (C) HAV virions were incubated with increasing amounts of D1muc-Fc (0.2, 2, 10, and 20 μg) for 2 h at 37°C and analyzed through 15 to 30% sucrose gradients as indicated above. The data shown are mean results from duplicate wells, and the standard deviations are shown as error bars. (D) A finer titration of the amount of D1muc-Fc (0.2, 0.5, 1, and 2 μg) needed to disrupt HAV particles was done with the same conditions described for panel C. Poliovirus native virions and empty particles labeled with [^{35}S]methionine were used as 160S and 80S sedimentation markers. The top and bottom of the gradients are indicated. OD, optical density.

HAV antibodies and subjected to Western blot analysis with staining with guinea pig anti-HAV antibodies (Fig. 6B). VP1 was detected in fractions 5 to 10 of the PVR-Fc gradient, which correlated with the peak of 160S particles detected by ELISA. Low levels of VP1 were detected in fractions 4 to 10 of the D1muc-Fc gradient, which may represent undisrupted residual 160S particles. VP1 bands were also observed in fractions 11 to 15 of the D1muc-Fc gradient, reaching a maximum level in fraction 13, which correlated with the peak of 100- to 125S particles detected by ELISA. We did not detect capsid subunits resulting from disruption of the viral particles at the top of the gradient, which agrees with our previous observation pointing to the instability of the viral subunits or their lack of reaction with the antibodies used in the assay. These data clearly indicate that the 100- to 125S particles were indeed HAV particles that most likely were altered by treatment with D1muc-Fc.

To determine whether the 100- to 125S particles contain HAV RNA, we quantitated the amount of viral RNA in the sucrose gradient fractions with a one-step real-time *Taq*Man RT-PCR assay (Fig. 7A). Fractions 4 to 6 and 10 to 12 of each gradient were pooled, and RNA was extracted, ethanol precipitated, and quantitated by the *Taq*Man assay in triplicates (Fig. 7B). In the PVR-Fc gradient, fractions 4 to 6 contained 8.83×10^5 copies of HAV RNA, which is consistent with the peak of virions, and fractions 10 to 12 contained 2.65×10^4 copies of HAV RNA, which was considered the background level of HAV RNA in the experiment. In the D1muc-Fc gradient, fractions 4 to 6 contained only 3.15×10^4 copies of HAV

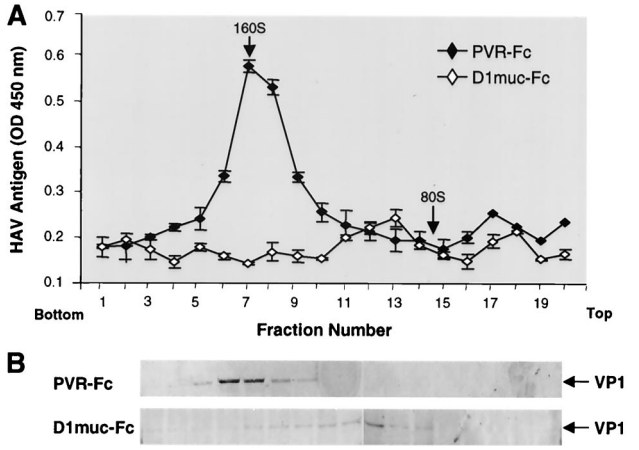

FIG. 6. Western blot analysis of 100- to 125S HAV particles. (A) Purified cytopathic HAV virions were treated with 10 μg of D1muc-Fc or PVR-Fc and sedimented through 15 to 30% sucrose gradients at 4°C for 90 min with an SW40 rotor at 40,000 rpm. Gradients were collected from the bottom in 20 fractions. HAV antigen in the fractions was determined by capture ELISA. (B) Fractions 4 to 20 of the gradients were incubated with rabbit anti-HAV antibodies and magnetic beads coated with anti-rabbit IgG for 2 h at 4°C. After extensive washing, the beads were boiled in denaturing buffer and proteins were studied by Western blot analysis with staining with guinea pig anti-HAV antibodies and phosphatase-labeled goat anti-guinea pig antibodies. The arrows point to the VP1 structural protein of HAV. The top and bottom of the gradients are indicated. OD, optical density.

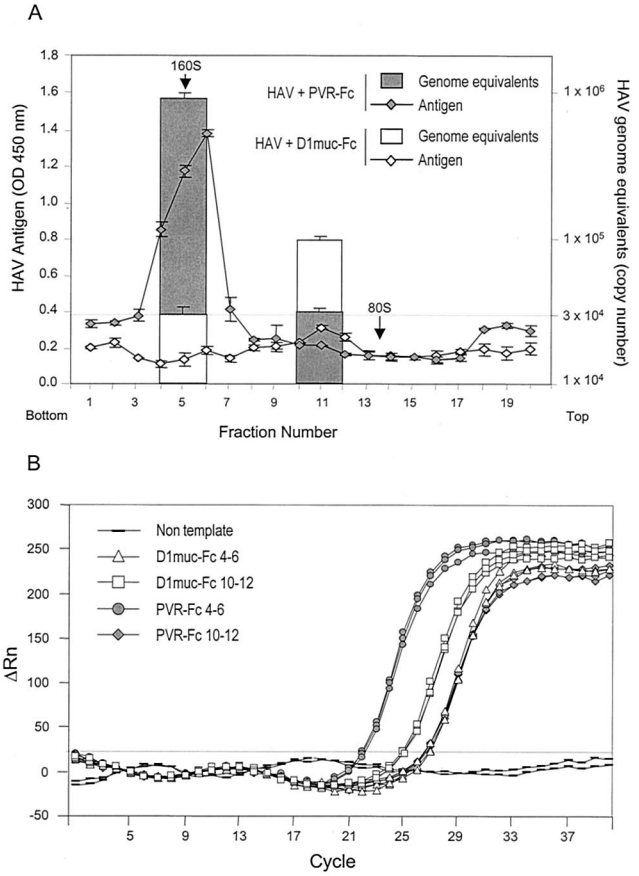

FIG. 7. Quantification of HAV RNA in 100- to 125S particles. (A) Purified HAV virions were incubated with 10 μg of D1muc-Fc or PVR-Fc for 2 h at 37°C and analyzed through 15 to 30% sucrose gradients as described in the legend to Fig. 6. Fractions containing HAV particles (4 to 6 and 10 to 12) were pooled, and RNA was extracted, ethanol precipitated, and quantitated with a one-step real-time *Taq*Man RT-PCR assay. In vitro-synthesized full-length HAV RNA was used as the standard for the quantitative PCR. The data shown are mean results from triplicate reactions. Standard deviations are shown as error bars. Poliovirus particles labeled with [^{35}S]methionine were used as 160S and 80S sedimentation markers. The top and bottom of the gradient are indicated. (B) *Taq*Man amplification plot of each triplicate reaction used to calculate the mean number of HAV genome equivalents in panel A. The ΔRn (increment of fluorescence reporter signal) for each sample was plotted against the cycle number. OD, optical density.

RNA, which is consistent with the lack of virions resulting from the soluble-receptor-mediated disruption of the viral particles. Fractions 10 to 12 of the same gradient contained 9.53×10^4 copies of RNA, which is significantly higher than the background level of RNA and indicative of the association of the 100- to 125S particles with genomic RNA.

Characterization of HAV particles by EM. HAV particles were further characterized by EM analysis with negative staining. A partially purified preparation of strain HM175 of HAV that contained 80S particles was treated with 10 μg of D1muc-Fc or PVR-Fc and analyzed in 15 to 30% sucrose gradients. Fractions from five parallel D1muc-Fc sucrose gradients were pooled, concentrated, and washed. Fractions from the PVR-Fc gradient were also concentrated and washed. HAV particles were negatively stained with 2% uranyl acetate and observed under the electron microscope (Fig. 8A to C). In the PVR-Fc gradient, we observed the characteristic 160S refringent virions (A) with well-defined edges, as well as a small proportion of 80S empty particles (B) with a doughnut shape and heavily stained centers. Although the EM images are somewhat grainy, they suggest that the 100- to 125S fractions of the D1muc-Fc gradients contain particles with internal staining (C), which is characteristic of altered virions that allowed the penetration of the negative stain. These altered particles also showed poorly defined edges that suggested the presence of bound receptors.

To study the kinetics of the receptor-mediated disruption of HAV, purified KRM003 HAV virions were treated with D1muc-Fc, negatively stained without sedimentation through sucrose gradients, and analyzed by EM (Fig. 8D to F). These EM images are presented at a lower resolution to show that the disruption of the HAV particles described in Fig. 5 was not restricted to a few particles in the preparation. As expected, the amount of disrupted HAV particles increased with the time of incubation. At 10 min postincubation, the majority of the particles were of uniform size and highly refringent (D). At 30 min postincubation, most of the particles were internally stained and not refringent (E), which indicated that the majority of the virions were disrupted by the soluble-receptor treatment. In addition, we observed the appearance of small protein clusters most likely derived from broken particles. At 60 min postincubation, we observed a significant reduction in the overall number of particles and the absence of refringent particles (F), which is consistent with the complete disruption

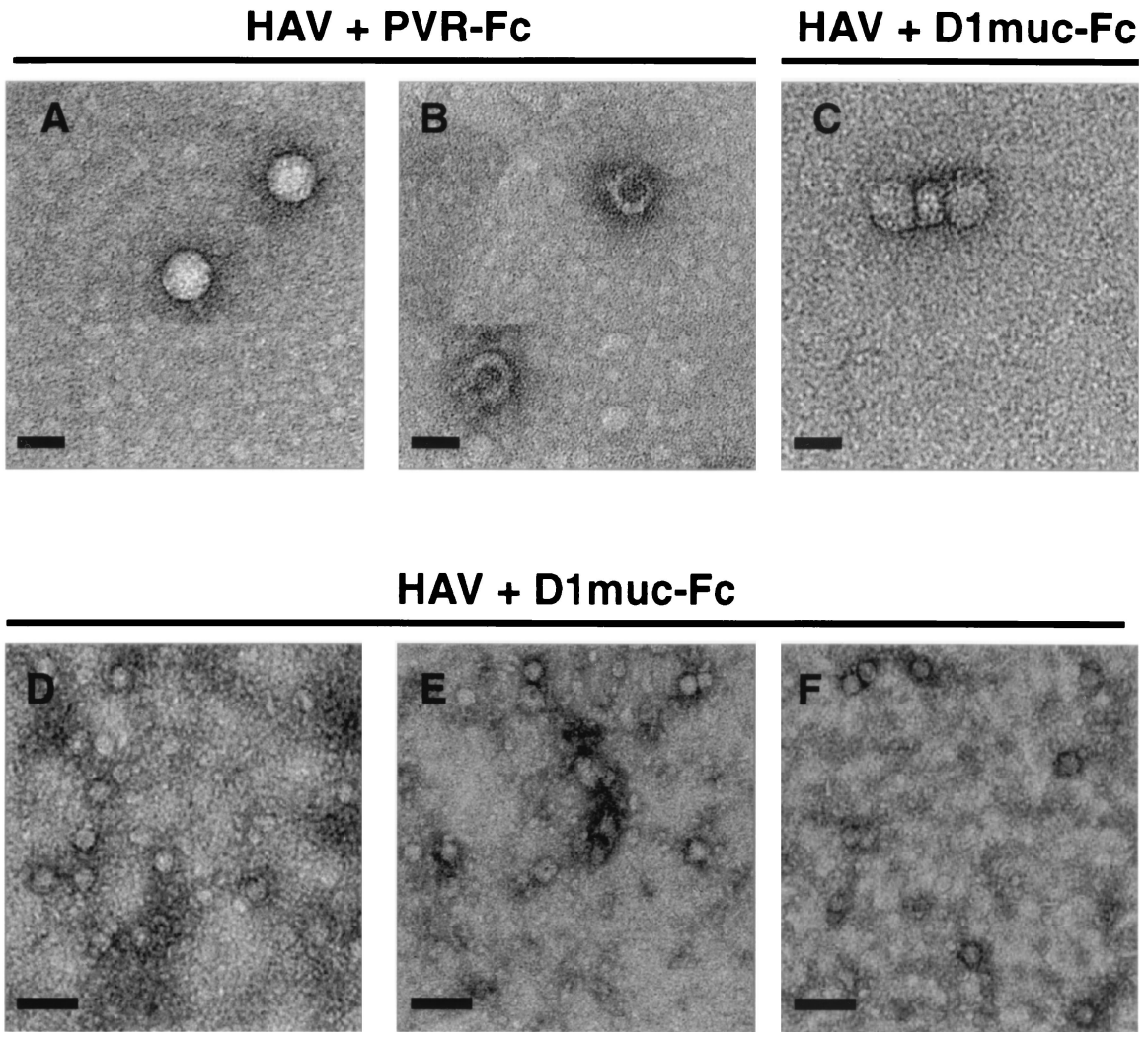

FIG. 8. Negative-stain EM analysis of HAV particles. HAV was incubated with 10 μg of D1muc-Fc or PVR-Fc for 2 h at 37°C and analyzed through 15 to 30% sucrose gradients as described in the legend to Fig. 6. Fractions containing the 100- to 125S particles from five D1muc-Fc sucrose gradients were pooled and concentrated. Fractions containing 160S and 80S HAV particles from one PVR-Fc sucrose gradient were pooled and concentrated. HAV virions (A), empty capsids (B), and 100- to 125S particles (C) were bound to grids, stained with 2% uranyl acetate, and analyzed by EM at a magnification of ×45,000. Purified KRM003 HAV virions were treated with 30 μg of D1muc-Fc for 10 (D), 30 (E), and 60 (F) min, stained directly without sedimentation, and analyzed by EM at a magnification of ×17,000. Bars: A, B, and C, 30 nm; D, E, and F, 100 nm.

of the HAV virions observed in the sedimentation experiments. Interestingly, treatment of HAV with D1muc-Fc did not result in aggregation of the altered particles (Fig. 8D to E). Therefore, it is likely that the concentration and washing steps of the sucrose gradient fractions, which were required for the EM analysis, were responsible for the aggregation of the HAV particles shown in Fig. 8C. Our EM analysis further suggested that the 100- to 125S particles are altered HAV virions that contain genomic RNA and possibly bound soluble receptors and suggested that these particles represent uncoating intermediates.

DISCUSSION

Crucial steps of the cell entry mechanism of picornaviruses are poorly understood despite the intensive work in the field. Cellular receptors for several members of the family *Picornaviridae* have been isolated and extensively studied. However, the steps following, binding to cellular receptors which lead to uncoating of the viral genome and its delivery to the cytoplasm are still a black box. Although picornaviruses are genetically and structurally related, the mechanism of cell entry differs substantially among members of the family. For instance, poliovirus type 1 is likely to uncoat at the cell surface (1, 23) whereas human rhinovirus 2 requires endocytosis (33). HAV is an atypical picornavirus that grows poorly in cell culture, which increases the complexity of the work and resulted in a poor understanding of its mechanism of cell entry. Elegant experiments of classical virology defined some of the elements of the cell entry process of HAV (3–6). However, a more detailed understanding at the molecular level is required to build a model of HAV cell entry. We have undertaken genetic and bio-

chemical approaches to understand the cell entry of HAV and have identified havcr-1 (24) and its human homolog huhavcr-1 (16) as cellular receptors for HAV. We have also shown that D1, the N-terminal cysteine-rich Ig-like region of havcr-1, is required for HAV receptor function (35) and is sufficient for binding and neutralization of HAV (34). However, binding and neutralization of HAV by a soluble-receptor construct containing only D1 was poor and suggested that the mucin-like region of havcr-1 could play a role in HAV receptor function. To further characterize the HAV–havcr-1 interaction, we constructed D1muc-Fc, a soluble receptor form containing D1 plus two-thirds of the mucin-like region of havcr-1 fused to the hinge and Fc regions of human IgG1. Interestingly, D1muc-Fc neutralized HAV more efficiently than did D1-Fc (Fig. 3), a similar construct that does not contain the mucin-like region of havcr-1. Although D1 is necessary and sufficient for HAV binding, the mucin-like region of havcr-1 seems to play a major role in the virus-receptor interaction leading to uncoating of the viral genome. Our experiments showed that treatment of HAV with D1muc-Fc had a major effect on the sedimentation profile of HAV and resulted in disruption of the viral particles (Fig. 5B), whereas treatment with D1-Fc had a minor effect on the sedimentation profile of the virions (Fig. 5A). Therefore, it is likely that the inefficient HAV neutralization induced by D1-Fc (34) resulted from blocking of virus-receptor binding sites whereas the efficient neutralization induced by D1muc-Fc resulted from disruption of HAV infectious particles. Although the exact function of the mucin-like region is still undetermined, our results indicated that it plays a role in HAV uncoating, perhaps providing adequate scaffolding for D1 presentation or interacting directly with the viral particles.

Uncoating intermediates have been isolated and characterized for some picornaviruses (for a review, see reference 32) but not for HAV. A particles, postulated as uncoating intermediates in some picornaviruses such as poliovirus and rhinovirus but not foot-and-mouth disease virus, have not been found in HAV (4). However, dense particles that cosediment with 160S virions but are permeable to CsCl and sensitive to RNases, have been postulated as HAV uncoating intermediates (4 and references therein). The relationship between the HAV dense particles and the 100- to 125S particles described in this paper is unknown, and it will be interesting to determine whether the dense particles are precursors to the 100- to 125S particles. Under our experimental conditions, 10 nM D1muc-Fc disrupted almost all HAV virions and resulted in low-level accumulation of 100- to 125S HAV particles (Fig. 5 and 6) that are associated with viral RNA (Fig. 7). This accumulation of the 100- to 125S particles seems to be dependent on the concentration of D1muc-Fc. However, it is not clear why the 100- to 125S particles are preferentially accumulated when 10 μg of D1muc-Fc is used in the reaction mixture. The conditions and requirements for the alteration of HAV and accumulation of the 100- to 125S particles, such as temperature, pH, and the presence of monovalent and divalent cations, are unknown but are under investigation. EM analysis showed that negative stain penetrated the 100- to 125S particles (Fig. 8), which is characteristic of altered virions. It is tantalizing to speculate that these 100- to 125S particles represent uncoating intermediates of HAV. Further research is required to determine whether the 100- to 125S particles are truly uncoating intermediates. The data presented in this paper will help in the development of a model of cell entry by HAV.

ACKNOWLEDGMENTS

This work was supported by funding from the Food and Drug Administration and the Karolinska Institute.

REFERENCES

1. **Belnap, D. M., D. J. Filman, B. L. Trus, N. Cheng, F. P. Booy, J. F. Conway, S. Curry, C. N. Hiremath, S. K. Tsang, A. C. Steven, and J. M. Hogle.** 2000. Molecular tectonic model of virus structural transitions: the putative cell entry states of poliovirus. J. Virol. **74:**1342–1354.
2. **Belnap, D. M., B. M. McDermott, Jr., D. J. Filman, N. Cheng, B. L. Trus, H. J. Zuccola, V. R. Racaniello, J. M. Hogle, and A. C. Steven.** 2000. Three-dimensional structure of poliovirus receptor bound to poliovirus. Proc. Natl. Acad. Sci. USA **97:**73–78.
3. **Bishop, N. E.** 1999. Effect of low pH on the hepatitis A virus maturation cleavage. Acta Virol. **43:**291–296.
4. **Bishop, N. E.** 2000. Hepatitis A virus replication: an intermediate in the uncoating process. Intervirology **43:**36–47.
5. **Bishop, N. E., and D. A. Anderson.** 1997. Early interactions of hepatitis A virus with cultured cells: viral elution and the effect of pH and calcium ions. Arch. Virol. **142:**2161–2178.
6. **Bishop, N. E., and D. A. Anderson.** 2000. Uncoating of hepatitis A virus virions and provirions. J. Virol. **74:**3423–3426.
7. **Cohen, J. I., B. Rosenblum, S. M. Feinstone, J. Ticehurst, and R. H. Purcell.** 1989. Attenuation and cell culture adaptation of hepatitis A virus (HAV): a genetic analysis with HAV cDNA. J. Virol. **63:**5364–5370.
8. **Cohen, J. I., B. Rosenblum, J. R. Ticehurst, R. J. Daemer, S. M. Feinstone, and R. H. Purcell.** 1987. Complete nucleotide sequence of an attenuated hepatitis A virus: comparison with wild-type virus. Proc. Natl. Acad. Sci. USA **84:**2497–2501.
9. **Cromeans, T., M. D. Sobsey, and H. A. Fields.** 1987. Development of a plaque assay for a cytopathic, rapidly replicating isolate of hepatitis A virus. J. Med. Virol. **22:**45–56.
10. **Daemer, R. J., S. M. Feinstone, I. D. Gust, and R. H. Purcell.** 1981. Propagation of human hepatitis A virus in African green monkey kidney cell culture: primary isolation and serial passage. Infect Immun. **32:**388–393.
11. **Dotzauer, A., S. M. Feinstone, and G. Kaplan.** 1994. Susceptibility of nonprimate cell lines to hepatitis A virus infection. J. Virol. **68:**6064–6068.
12. **Emerson, S. U., Y. K. Huang, and R. H. Purcell.** 1993. 2B and 2C mutations are essential but mutations throughout the genome of HAV contribute to adaptation to cell culture. Virology **194:**475–480.
13. **Emerson, S. U., Y. K. Huang, C. McRill, M. Lewis, and R. H. Purcell.** 1992. Mutations in both the 2B and 2C genes of hepatitis A virus are involved in adaptation to growth in cell culture. J. Virol. **66:**650–654.
14. **Emerson, S. U., Y. K. Huang, C. McRill, M. Lewis, M. Shapiro, W. T. London, and R. H. Purcell.** 1992. Molecular basis of virulence and growth of hepatitis A virus in cell culture. Vaccine **10:**S36–S39.
15. **Feigelstock, D., P. Thompson, P. Mattoo, and G. G. Kaplan.** 1998. Polymorphisms of the hepatitis A virus cellular receptor 1 in African green monkey kidney cells result in antigenic variants that do not react with protective monoclonal antibody 190/4. J. Virol. **72:**6218–6222.
16. **Feigelstock, D., P. Thompson, P. Mattoo, Y. Zhang, and G. G. Kaplan.** 1998. The human homolog of HAVcr-1 codes for a hepatitis A virus cellular receptor. J. Virol. **72:**6621–6628.
17. **Funkhouser, A. W., R. H. Purcell, E. D'Hondt, and S. U. Emerson.** 1994. Attenuated hepatitis A virus: genetic determinants of adaptation to growth in MRC-5 cells. J. Virol. **68:**148–157.
18. **He, Y., V. D. Bowman, S. Mueller, C. M. Bator, J. Bella, X. Peng, T. S. Baker, E. Wimmer, R. J. Kuhn, and M. G. Rossmann.** 2000. Interaction of the poliovirus receptor with poliovirus. Proc. Natl. Acad. Sci. USA **97:**79–84.
19. **Hewat, E., E. Neumann, J. F. Conway, R. Moser, B. Ronacher, T. C. Marlovits, and D. Blass.** 2000. The cellular receptor to human rhinovirus 2 binds around the 5-fold axis and not in the canyon: a structural view. EMBO J. **19:**6317–6325.
20. **Hollinger, F. B., and S. U. Emerson.** 2001. Hepatitis A virus, p. 799–840. *In* B. N. Fields, D. M. Knipe, and P. M. Howley (ed.), Fields virology. Raven Press, New York, N.Y.
21. **Jackson, T., A. Sharma, R. Abu-Ghazaleh, W. E. Blakemore, F. M. Ellard, D. L. Simmons, J. W. I. Newman, D. I. Stuart, and A. M. Q. King.** 1994. Arginine-glycine-aspartic acid-specific binding of foot-and-mouth disease virus to the purified integrin αvβ3 in vitro. J. Virol. **71:**8357–8361.
22. **Kaplan, G., D. Peters, and V. R. Racaniello.** 1990. Poliovirus mutants resistant to neutralization with soluble cell receptors. Science **250:**1596–1609.
23. **Kaplan, G., M. S. Freistadt, and V. R. Racaniello.** 1990. Neutralization of poliovirus by cell receptors expressed in insect cells. J. Virol. **64:**4697–4702.

24. **Kaplan, G., A. Totsuka, P. Thompson, T. Akatsuka, Y. Moritsugu, and S. M. Feinstone.** 1996. Identification of a surface glycoprotein on African green monkey kidney cells as a receptor for hepatitis A virus. EMBO J. **15:**4282–4296.
25. **Matricardi, P., F. Rosmini, L. Ferrigno, R. Nisini, M. Rapicetta, P. Chionne, T. Stroffolini, P. Pasquini, and R. D'Amelio.** 1997. Cross sectional retrospective study of prevalence of atopy among Italian military students with antibodies against hepatitis A virus. Br. J. Med. **314:**999–1003.
26. **Matricardi, P. M., F. Rosmini, V. Panetta, L. Ferrigno, and S. Bonini.** 2002. Hay fever and asthma in relation to markers of infection in the United States. J. Allergy Clin. Immunol. **110:**381–387.
27. **McIntire, J., S. E. Umetsu, A. Omid, M. Potter, V. K. Kuchroo, G. S. Barsh, G. J. Freeman, D. T. Umetsu, and R. H. DeKruyff.** 2001. Identification of Tapr (an airway hyperreactivity regulatory locus) and the linked Tim gene family. Nat. Immunol. **2:**1109–1116.
28. **Miller, L. C., W. Blakemore, D. Sheppard, A. Atakilit, A. M. Q. King, and T. Jackson.** 2001. Role of the cytoplasmic domain of the β-subunit of integrin αvβ6 in infection of foot-and-mouth disease virus. J. Virol. **75:**4158–4164.
29. **Probst, C., M. Jecht, and V. Gauss-Muller.** 1999. Intrinsic signals for the assembly of hepatitis A virus particles. J. Biol. Chem. **274:**4527–4531.
30. **Provost, P. J., and M. R. Hilleman.** 1979. Propagation of human hepatitis A virus in cell culture in vitro. Proc. Soc. Exp. Biol. Med. **160:**213–221.
31. **Reed, L. J., and H. Muench.** 1938. A simple method of estimating fifty per cent endpoints. Am. J. Hyg. **27:**493–497.
32. **Rossmann, M. G., Y. He, and R. J. Kuhn.** 2002. Picornavirus-receptor interactions. Trends Microbiol. **10:**324–331.
33. **Schober, D., P. Kronenberger, E. Prchla, D. Blaas, and R. Fuchs.** 1998. Major and minor receptor group human rhinoviruses penetrate from endosomes by different mechanisms. J. Virol. **72:**1354–1364.
34. **Silberstein, E., G. Dveksler, and G. G. Kaplan.** 2001. Neutralization of hepatitis A virus (HAV) by an immunoadhesin containing the cysteine-rich region of HAV cellular receptor-1. J. Virol. **75:**717–725.
35. **Thompson, P., J. Lu, and G. G. Kaplan.** 1998. The Cys-rich region of hepatitis A virus cellular receptor 1 is required for binding of hepatitis A virus and protective monoclonal antibody 190/4. J. Virol. **72:**3751–3761.
36. **Totsuka, A., and Y. Moritsugu.** 1994. Hepatitis A vaccine development in Japan, p. 509–513. *In* K. Nishioka, H. Suzuki, S. Mishiro, and T. Oda (ed.), Viral hepatitis and liver disease. Springer Verlag, Tokyo, Japan.
37. **Umetsu, D. T., J. J. McIntire, O. Akbari, C. Macaubas, and R. H. DeKruyff.** 2002. Asthma: an epidemic of dysregulated immunity. Nat. Immunol. **3:**715–720.
38. **Weitz, M., B. M. Baroudy, W. L. Maloy, J. R. Ticehurst, and R. H. Purcell.** 1986. Detection of a genome-linked protein (VPg) of hepatitis A virus and its comparison with other picornaviral VPgs. J. Virol. **60:**124–130.
39. **Xing, L., K. Tjarnlund, B. Lindqvist, G. G. Kaplan, D. Feigelstock, R. H. Cheng, and J. M. Casasnovas.** 2000. Distinct cellular receptor interactions in poliovirus and rhinoviruses. EMBO J. **19:**1207–1216.
40. **Zhang, Y., and G. G. Kaplan.** 1998. Characterization of replication-competent hepatitis A virus constructs containing insertions at the N terminus of the polyprotein. J. Virol. **72:**349–357.